Physica B: Condensed Matter 531 (2018) 30–34

Contents lists available at ScienceDirect

Physica B: Condensed Matter

journal homepage: www.elsevier.com/locate/physb

Size-controlled heating ability of $CoFe_2O_4$ nanoparticles for hyperthermia applications

P.T. Phong [a,b,*], N.X. Phuc [c], P.H. Nam [d,e], N.V. Chien [d], D.D. Dung [f], P.H. Linh [d,**]

[a] Theoretical Physics Research Group, Ton Duc Thang University, Ho Chi Minh City, Viet Nam
[b] Faculty of Applied Sciences, Ton Duc Thang University, Ho Chi Minh City, Viet Nam
[c] Duy Tan University, K7/25 Quang Trung, Da Nang, Viet Nam
[d] Institute of Materials Science, Vietnam Academy of Science and Technology, 18- Hoang Quoc Viet Street, Cau Giay District, Ha Noi City, Viet Nam
[e] Graduate University of Science and Technology, Vietnam Academy of Science and Technology, 18 Hoang Quoc Viet, Hanoi, Viet Nam
[f] School of Engineering Physics, Ha Noi University of Science and Technology, Dai Co Viet Road, Ha Noi City, Viet Nam

ARTICLE INFO

Keywords:
$CoFe_2O_4$ nanoparticles
Magnetic hyperthermia
Magnetic nanofluid
Specific absorption rate
Nanomedicine

ABSTRACT

The magnetic properties and heating capacity of cobalt ferrite ($CoFe_2O_4$) nanoparticles 13–24 nm in size were studied. Results showed that the specific absorption rate of the nanoparticles strongly depended on their magnetic properties and particle size. Specific absorption rate values decreased with increased particle size, and the smallest $CoFe_2O_4$ nanoparticles (13.5 nm) exhibited the highest specific absorption rate. The mechanism underlying the decrease in specific absorption rate of the $CoFe_2O_4$ nanoparticles with increased particle size was also discussed.

1. Introduction

Magnetic nanoparticles (MNPs) are attracting research attention because their unique physical properties have potential significant uses in various biomedical applications [1–5]. In particular, MNPs can generate heat in an alternating magnetic field and are promising heating mediators in magnetic hyperthermia, a cancer treatment strategy [6,7]. Magnetic hyperthermia is dominated by energy loss from the three main heating mechanisms of i) hysteresis loss, ii) Néel relaxation loss, and iii) Brown relaxation loss [8,9]. The heat dissipation of superparamagnetic nanoparticles (NPs) is seldom accompanied by hysteresis loss, whereas ferromagnetic NPs exhibit significant hysteresis loss that is expected to improve heating efficiency. Thus, ferromagnetic NPs are crucial in generating high hysteresis loss. However, the individual effects of material parameters (e.g., particle size, coercivity (H_c), magnetic anisotropy, and dipolar interaction) on each heating mechanism remain unclear because of the simultaneous contribution of the three aforementioned mechanisms. Thus, the key mechanism underlying heat dissipation should first be identified. In addition, optimizing particle size to obtain the maximum specific loss power has not been realized and the influence of NPs interaction on magnetic heating capacity needs to be clarified. The control of particle sizes, which dramatically changes both the Néel and Brownian relaxation times as well as hysteresis loss, manages the heating power [10]. The heat generation is reduced as size distribution increased. Heating efficiency, often denoted as specific absorption rate (SAR), is directly related to the heat losses of the MNPs when exposed to the AC field [11]. Therefore, the SAR is related to the particle size, the solvent type, and the particle size distribution. In addition, magnetic NPs need to be monodispersed in Magnetic Fluid Hyperthermia applications for controllable temperature increase; therefore, a low amount of magnetic particles should be used, decreasing the possibility of contaminating cells [12,13]. $CoFe_2O_4$ NPs have received renewed attention for their use in recording media, memory cores, and high-frequency devices because of their unique magnetic, electronic, optical, and physical properties, such as high Curie temperature, large magnetocrystalline anisotropy, large magnetostrictive coefficient, and excellent chemical stability [14]. Several studies have revealed that $CoFe_2O_4$ NPs offer some advantage in the future enhancement of hyperthermia heating [9,13,15–18]. *In vitro* and *in vivo* studies on $CoFe_2O_4$ demonstrated that it can be used as a bio-material for magnetic hyperthermia application [19,20]. Therefore, in the past few years, numerous studies have been conducted to determine the natural biocompatibility and the hyperthermia application of cobalt ferrites [15–18].

* Corresponding author. Ton Duc Thang University, Ho Chi Minh City, Viet Nam.
** Corresponding author.
E-mail addresses: phamthanhphong@tdt.edu.vn (P.T. Phong), linhph.ims@gmail.com (P.H. Linh).

https://doi.org/10.1016/j.physb.2017.12.010
Received 4 September 2017; Received in revised form 3 December 2017; Accepted 4 December 2017
Available online 6 December 2017

In consideration of all the above mentioned issues, we fabricated $CoFe_2O_4$ NPs with controlled sizes using a chemical method. Then, the effects of particle size on the magnetic properties and magnetic heating capacity of the synthesized $CoFe_2O_4$ NPs were investigated. This work also investigated the influence of coercive and magnetic relaxation processes on the heating efficiency of the $CoFe_2O_4$ NPs.

2. Experimental

$CoFe_2O_4$ NPs with various sizes were synthesized using the microwave-assisted co-precipitation method. In the synthesis procedure, raw $FeCl_3{\cdot}H_2O$ and $CoCl_2{\cdot}4H_2O$ materials were dissolved in a three-necked flask containing 2 M HCl solution under vigorous stirring. The mixed solution was rapidly heated by controlled power microwave irradiation, and then sodium hydroxide NaOH (1.5 M) solution was added to the mixed solution until the pH of the solution reached 11. The temperature was maintained at 80 °C, 100 °C, and 160 °C during the reaction process, which lasted 15 min. After the reaction finished, the solution containing the formed $CoFe_2O_4$ NPs was obtained. The samples were defined as Co1 and Co2 corresponding to the reaction temperature at 80 °C and 100 °C. The Co3 was obtained by using the resulting product of Co2 sample for the next hydrothermal step. Half of the resulting product of the Co2 sample was transferred into a Teflon-lined stainless steel autoclave, and then the autoclave was heated up to 160 °C, maintaining the whole system at this temperature for 8 h. Once reaction time was completed, the autoclave was cooled down to room temperature. Finally, a solution containing $CoFe_2O_4$ NPs of all samples was separated and washed several times by magnetic decantation and deionized water. The final product was dried at 60 °C for 8 h.

The structures and crystalline sizes of the samples were investigated by X-ray diffraction (SIEMENS D5000) with Cu–Kα radiation ($\lambda = 1.5406$ Å) in the 2theta from 10° to 80°. Shape and distribution of particles were investigated by Transmission Electron Microscopy (TEM 1010—JEOL). A vibrating sample magnetometer (VSM- MicroSence EZ9) was used to observe magnetic properties, such as superparamagnetic behavior and saturation magnetization. The hysteresis loops and zero field cooling and field cooling measurements were performed under the applied field of up to 18 kOe and a temperature in the range of 70–600 K. The magnetic properties of the samples were investigated with a VSM. The heating efficiency of the samples was investigated on the basis of temperature–time curves under the alternating magnetic field source of a generator (RDO HFI 5 kW) with an amplitude of 40–100 Oe at a frequency of 170–240 kHz. In this process, the samples were dispersed in water medium with different concentrations (5, 2.5, and 1 mg/mL), then they were placed into a coil connected to a power generator. The temperature increase of the sample while the field is applied was recorded by a fiber optic temperature sensor. The SAR values and intrinsic loss power (ILP) of the prepared samples were determined through the Bekovic and Hamler method [21] by the given formula:

$$SAR = \frac{C_M m_M + C_{H_2O} m_{H_2O}}{m_M} \frac{dT}{dt} \quad (1)$$

where C_M and m_M are the specific heat capacity (0.67 J/gK) and mass of $CoFe_2O_4$; C_{H_2O} and m_{H_2O} are the specific heat capacity (4.18 J/gK) and mass of water, respectively; dT/dt is the initial temperature rising rate that was estimated by the method suggested by Bekovic and Hamler [21]. The $dT/dt = \Delta T_{max}/\tau$ where ΔT_{max} and τ are the temperature change from initial to steady state and the time constant of the heating. These parameters are obtained from fitting the experimental data of the heating curve to a function that describes the increasing temperature process: $T(t) = T_{initial} + \Delta T_{max}(1 - exp(-t/\tau))$. The ILP was introduced as the following equation:

$$ILP = \frac{SAR}{H^2 f} \quad (2)$$

where H is the strength of magnetic field and f (Hz) is the field frequency. In this study, the alternating magnetic field with a strength of 80 Oe and frequency of 178 kHz was applied.

3. Results and discussion

Fig. 1 shows the XRD patterns of all samples. The relative peaks of XRD patterns such as: (111), (220), (311), (400), (422), (511) correspond to the inverse cubic spinel structure of cobalt ferrite which matches well with JPCDS standard card number 01-074-3419 without undesired impurities. The average crystalline size of $CoFe_2O_4$ NPs can be calculated by using Scherrer's equation.

$$d = \frac{0.9\lambda}{\beta \cos\theta} \quad (3)$$

where λ is the wavelength of radiation, β is full width at half maximum which was determined from the experimental integral peak width of the (311) peak, θ is Bragg angle. The average crystalline sizes of Co1, Co2, and Co3 samples were calculated to be 12.8, 16.1, and 22.3 nm, respectively.

Fig. 2 shows the TEM images and size distribution of the obtained $CoFe_2O_4$ NPs. The $CoFe_2O_4$ NPs exhibit nearly spherical shape with uniform size. The frequency of particle sizes was determined by measuring the diameter of 150 particles based on TEM images. By fitting with the Lognormal distribution function, we found that the average particle sizes of the Co1, Co2, and Co3 samples were approximately 13.5 ± 2.2, 17.8 ± 2.5, and 24.2 ± 4.1 nm, respectively. These results are in good agreement with the crystallite size inferred from the XRD patterns. Therefore, single crystalline $CoFe_2O_4$ NPs with various sizes were successfully synthesized.

Fig. 3 shows the magnetization versus applied magnetic field (M–H) curves of the samples at room temperature. The results provided solid evidence for the size-controlled magnetic behavior of the $CoFe_2O_4$ NPs. Saturation magnetization (M_s) decreased as the particle sizes decreased. In addition, the magnified central region of the M–H curves (inset of Fig. 3), indicated that the curves broadened with increased particle size. The H_C values for Co1, Co2, and Co3 samples were approximately 43, 378, and 850 Oe, respectively. The M_S values of Co1, Co2, and Co3 samples were extrapolated from the initial magnetization curves through the fitting of the experimental data at high applied field under the law of approach to saturation [22], which can be written as:

$$M = M_s\left(1 - \frac{a}{H} - \frac{b}{H^2} - \cdots\right) + \chi_p H \quad (4)$$

The best fitting of the magnetization curves using Eq. (2) is shown in Fig. 4 for all samples by considering M_s, a, and b as free parameters. The

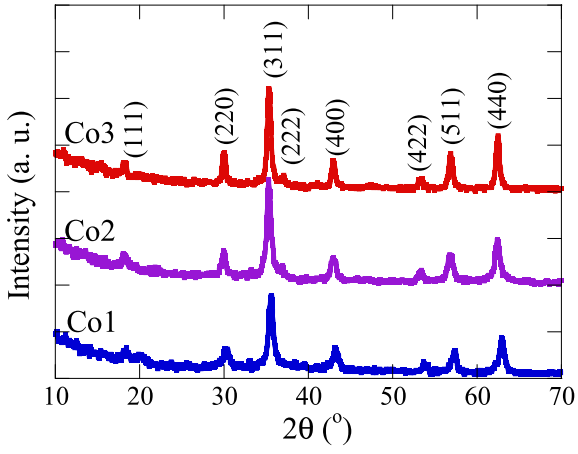

Fig. 1. X-ray diffraction patterns of $CoFe_2O_4$ NPs with different size.